We are IntechOpen,
the world's leading publisher of
Open Access books
Built by scientists, for scientists

6,900
Open access books available

186,000
International authors and editors

200M
Downloads

154
Countries delivered to

Our authors are among the

TOP 1%
most cited scientists

12.2%
Contributors from top 500 universities

WEB OF SCIENCE™

Selection of our books indexed in the Book Citation Index
in Web of Science™ Core Collection (BKCI)

Interested in publishing with us?
Contact book.department@intechopen.com

Numbers displayed above are based on latest data collected.
For more information visit www.intechopen.com

Linear and Nonlinear Synchronization Analysis and Visualization during Altered States of Consciousness

Vangelis Sakkalis[1] and Michalis Zervakis[2]
[1] Institute of Computer Science, Foundation for Research and Technology, Greece
[2] Electronic and Computer Engineering Dept., Technical University of Crete, Greece

1. Introduction

This chapter focuses on analyzing various established approaches in bio-medical signal analysis, with emphasis on the dynamic evolution of time series and their structural inter-relationships. The application area involves electroencephalographic (EEG) signals, but the analytic approaches can be extended to most physiological signals. Two major approaches will be discussed including i) linear synchronization methods and ii) nonlinear synchronization methods based on chaos theory. Comparisons and extensions will be thoroughly investigated as to highlight their advantages and limitations over traditional power-based techniques. In particular, this chapter will investigate traditionally formulated coherence methods (i.e., correlation, coherence, short time Fourier transform coherence) and modern linear analysis techniques (i.e., Wavelet coherence and the Partial Directed Coherence), as well as established nonlinear methods, such as phase and generalized synchronization algorithms. Applications will be referenced in the domains of cognitive awareness assessment and diagnosis of pathological cases, such as Schizophrenia, Alcoholism and Epilepsy. Furthermore, a link to graph theory and visualization of synchronization status will be briefly addressed in an attempt to better describe the functional characteristics of brain networks.

2. Linear synchronization techniques applied in EEG analysis

The revolutionary discoveries of Jean Baptiste Fourier (1768-1830), have had a major impact on the development of mathematics and are of great importance in an extremely wide range of scientific and engineering disciplines. Although, the original work of Fourier was focused on problems of mathematical Physics, which happen in the continuous time domain, there is also a rich variety of applications of the tools of Fourier analysis for discrete-time signals and systems. In particular, discrete-time concepts and methods are fundamental to the discipline of numerical analysis. Formulas for the processing of discrete sets of data points to produce numerical approximations for interpolation, integration, and differentiation were investigated in the early 1600's. This section starts with the mathematical foundation of the

traditionally formulated Magnitude Squared Coherence (MSCOH) that is based on the Fast Fourier Transform (FFT) theoretical foundation and extents to the most modern Wavelet and Partial Directed Coherence (PDC) ones.

2.1 Cross-correlation & Coherence

The study of functional relationships between two brain regions has been one of the main aims of the EEG. As early as 1951, the cross-correlation function was used to study the similarity between two EEG signals (Brazier and Casby, 1952). Its application in the area of brain analysis is based on the assumption that the higher the correlation, the stronger the functional relationships between the related brain regions (Shaw, 1981; Shaw, 1984). It has been extensively used in studying the interrelationships between different cortical regions in relation to sensory stimulation, voluntary movements, effect of drugs and a wide range of clinical and cognitive problems and tasks.

However, since the development of FFT, correlation has been replaced by an alternative mathematical method, the coherence spectrum. The latter, in addition to the correlation information, has the advantage of showing the co-variation between two signals as a function of frequency, thus allowing the study of spatial correlations between different bands (Gevins, 1987; Guevara et al., 1995). Coherence studies have been successfully conducted in many fields, including those dealing with cognitive functions and psychiatric disorders (French and Beaumont, 1984). To mention a few key articles that reviewed the applications of coherence to neural data the reader is referenced to (Dumermuth and Molinari, 1991; French and Beaumont, 1984; Shaw, 1984; Thatcher et al., 1986; Zaveri et al., 1999). Especially in epileptic seizures (Sakkalis et al., 2008a) when an abnormal synchronization of neurons takes place, coherence appears to be an ideal tool for measuring it (Sakkalis et al., 2009).

Both methods, correlation and coherence, may be considered as equivalent in that they evaluate the degree of similarity between two signals. However, there are important differences between them. Coherence is calculated by dividing the numerical square of the cross-spectrum by the product of the autospectra (eq. 3). Since, it is a complex measure; it is sensitive to both a change in power and a change in phase relationships. Consequently, if either power or phase changes in one of the signals, the coherence value is affected. Another important difference is that the value of coherence for a single epoch is always one, regardless of the true phase relationship and the differences in power between the two signals (Bendat and Piersol, 1993).

Therefore, the sample cross spectrum S_{xy} between two time series is defined by calculating the product of the Fourier transformed series as follows:

$$S_{xy}(f_k) = X(f_k) \cdot Y^*(f_k) \tag{1}$$

The latter measures the linear cross correlation between the two signals for any given frequencies. In general, the correlation function requires normalization to produce an accurate estimate and is given by:

$$C_{xy}(\tau) = \frac{1}{N-\tau} \sum_{k=1}^{N-\tau} x(k+\tau)y(k) \tag{2}$$

where N is the total number of samples and τ the time lag between the signals. Taking the square of the cross spectrum normalized by the auto spectra of each signal defines the magnitude squared coherence or simply the coherence Γ^2_{xy} as follows:

$$\Gamma^2_{xy}(f_k) = \frac{\left|\langle S_{xy}(f_k)\rangle\right|^2}{\left|\langle S_{xx}(f_k)\rangle\right|\left|\langle S_{yy}(f_k)\rangle\right|} \tag{3}$$

where $\langle\cdot\rangle$ indicates average over a number of equal in length signal segments or epochs, the so-called averaged modified periodogram typically using Welch's method.

Over successive epochs the coherence measure is dependent on power and phase of the two signals along the epochs. If there is no variation over time in the original relationship between the two signals, the coherence value remains unity. This means that coherence does not give direct information on the true relationship between the two signals, but only on the stability of this relationship with respect to power asymmetry and phase relationship. Correlation, on the other hand, may be calculated over a single epoch or over several epochs and it is sensitive to both, phase and polarity, independently of amplitudes. The calculation of coherence involves squaring the signal, thus producing values which go from 0 (linearly independent signals for a given frequency) to 1 (maximum linear correlation in given frequency), and a loss in polarity information. By contrast, correlation is sensitive to polarity and its values go from – 1 (complete linear inverse correlation) to +1 (complete linear direct correlation), with $C_{xy}(\tau) = 0$ suggesting lack of linear interdependence for a given time lag τ. However, under normal physiological conditions, no strong and abrupt power asymmetries would be expected to occur. Thus, the influence of power on coherence should be negligible and results similar to those produced by correlation also would be expected for the coherence measures.

Additionally one is able to define the phase function of the coherence as:

$$\Phi_{xy}(f_k) = \arctan\frac{-\Im S_{xy}(f_k)}{\Re S_{xy}(f_k)} \tag{4}$$

where $\Im$ and $\Re$ denote the imaginary and real part. Phase measure is meaningful only in the case of significant coherence, when one is interested in estimating the time delay between the two signals (Brazier, 1972) according to:

$$\tau_{xy}(f_k) = \frac{\Phi_{xy}}{2\pi f_k} \tag{5}$$

where Φ_{xy} is the phase difference in degrees at a frequency f_k.

Important concerns and limitations

It should be noted that EEG represents a set of continuous voltage/time values and may therefore be considered as a multivariate time series that belongs to the category of stochastic processes which may be described by probability distributions. The concept of temporal stochastic process may be extended, in the case of the EEG, to the spatial domain (Nunez, 1995). The stochastic nature (temporal and spatial) of the EEG allows the use of correlation and coherence analyses which presuppose independence between successive points in time. However, a trade-off has to be made regarding the length of the data segment for analysis, which on one hand must be short enough to satisfy the condition of

stationarity (required from Fourier Transform) and on the other hand must be long enough to provide good frequency resolution. EEG on the contrary is highly non-stationary.

Another concern is that Fourier transform loses the information concerning the time evolution of the signal, which in certain cases maybe useful.

Finally, another important point to take into account is that coherence is very sensitive to fluctuations of linearity in phase, relatively less so to nonlinear fluctuations of amplitude, and completely insensitive to linear fluctuations in amplitude. This becomes obvious if one rewrites equation 3 in terms of polar coordinates:

$$\Gamma^2_{xy}(f_k) = \frac{\left|\left\langle X(f_k) \cdot Y^*(f_k) \right\rangle\right|^2}{\left|\left\langle X^2(f_k) \right\rangle\right|\left|\left\langle Y^2(f_k) \right\rangle\right|} = \frac{\left|\left\langle |XY| e^{i(\arg X - \arg Y)} \right\rangle\right|^2}{\left|\left\langle |X|^2 \right\rangle\right|\left|\left\langle |Y|^2 \right\rangle\right|} \tag{6}$$

Both amplitude and phase information are evaluated with regard to their contribution to linear dependence. The relative importance of amplitude and phase covariance in this index is not altogether clear (Lachaux et al., 1999; Varela et al., 2001). Therefore, some authors have argued that amplitude should not contribute to the final measure at all. Hence, the relationship between the phases without any influence of the amplitudes is better calculated by alternative methods, i.e. Phase Locking Value (PLV) as described in section 3.1. Just to elucidate on this; PLV is essentially the square root of equation 6 with all the moduli set to 1.

2.2 Short time Fourier transform Coherence

The coherence measure, as described in section 2.1, assumes stationarity of the signals and is completely insensitive to the changes in coupling over time. Thus, a short time Fourier transform (STFT) approach is better suited and generally used to generate auto- and cross spectrograms, which are in turn utilized to produce the so called "coherogram". The coherogram is coherence calculated around a number of time instants. It results in a three dimensional matrix of time and frequency versus coherence.

However, while the assumption of wide sense stationarity is removed, stationarity is still required within each time interval for which coherence is calculated. In practice one should carefully decide on the optimal section length (over which each coherence estimate is measured), window length and overlapping (within each coherence estimate), which affects the resolution of the coupling measure. Hence, the STFT approach requires a priori information about the coupling range in time and frequency, in order to allocate the time-frequency resolution. The latter is constrained by the uncertainty principle: the wider the windows, the better the frequency resolution, at the expense of timing information, and vice versa. Lachaux et al. (2002) presents in detail this approach as applied to single-trial brain signals.

2.3 Wavelet Coherence

Coherence analysis, as noted before, ignores in a sense the temporal structure of the signal, thus cannot convey any information on dynamically varying or short-time dependence between the signals. To overcome this limitation and the implicit assumption that the signal is a process that remains stationary in time, wavelet coherence (WC) has been proposed. In contrast to the short time Fourier transform, which is just an extension of the regular Fourier transform, the wavelet transform is inherently a time frequency signal analysis. Continuous wavelet transform is preferred over the discrete counterpart in this case, as well. Since the

coherence estimator is most strongly influenced by linearity in phase, the wavelet should be complex.

Here again, the conceptually simple wavelet basis used, is the Morlet wavelet. This modulated Gaussian kernel has a simple and very smooth spectrum that allows for easy interpretation of the results achieved. Initially the cross wavelet transform (XWT) of two time series x_n and y_n is defined as:

$$W_n^{XY}(s) = W_n^X(s)W_n^{Y*}(s) \tag{7}$$

where $W_n^X(s)$ and $W_n^Y(s)$ are the WT of signals X and Y, respectively and * denotes complex conjugation. Furthermore, the cross wavelet power may be defined as $\left|W_n^{XY}(s)\right|^2$. The complex argument $\arg(W_n^{XY}(s))$ may be explained as the local relative phase between the two time series in time frequency space.

If one closely follows equation 3, then the wavelet coherence R_n^2 of two signals comes naturally and may be defined as:

$$R_n^2(s) = \frac{\left|S(s^{-1}W_n^{XY}(s))\right|^2}{S\left(s^{-1}\left|W_n^X(s)\right|^2\right) \cdot S\left(s^{-1}\left|W_n^Y(s)\right|^2\right)} \tag{8}$$

where S is a smoothing operator in time S_t (The time smoothing uses a filter given by the absolute value of the wavelet function at each scale, normalized to have a total weight of unity. For the Morlet wavelet this is just a Gaussian ($e^{-t^2/2s^2}$) and scale S_s such as $S(W) = S_s(S_t(W_n(s)))$ which for the Morlet wavelet is given by a Gaussian and a boxcar filter of width equal to 0.6, (the scale-decorrelation length) respectively (Grinsted et al., 2004; Torrence and Compo, 1998):

$$S_t(W,s) = \left(W_n(s) * c_1^{-t^2/2s^2}\right) \tag{9}$$

$$S_s(W,n) = \left(W_n(s) * c_2 \prod(0.6s)\right) \tag{10}$$

where c_1 and c_2 are normalization constants and $\prod$ is the rectangle function. The squared WC time-frequency transformed scalogram is depicted in figure 1.

Note that the Schwarz inequality (given using the notation of norm, as explained under norms on inner product spaces, as $\left|\langle x, y \rangle\right| \le \|x\|\|y\|$) forces the wavelet coherence to take on a value between 0 and 1. Moreover, the wavelet coherence is also a function of both time and (scale) frequency, measuring the coupling across both variables. The fact that the wavelet transform uses a shorter window for higher frequencies, and a longer one for lower frequencies makes this approach more suited to quantifying time varying coherence. This is accomplished via a frequency-adaptive tiling of the time frequency plane. In contrast, the constant size windows, and summation segments of the STFT coherence, force it to have the same resolution over all frequencies.
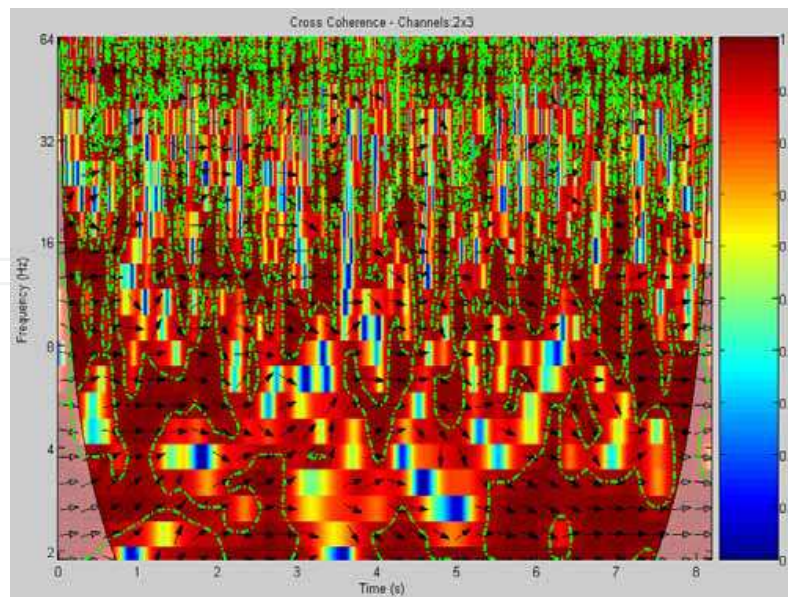
Fig. 1. The squared WC time-frequency transformed scalogram. The 5% significant regions over the time-scale transform are indicated by the contours (green dashed outline). The outer elliptical region at the edges of the second graph indicates the cone of influence in which errors (edge effects) may be apparent due to the transformation of a finite-length series EEG signal (Torrence and Compo, 1998). The relative phase relationship is shown as arrows (with in-phase pointing right, anti-phase pointing left).

In summary, the XWT identifies regions with high common power and can possibly convey information about the phase relationship. For example, if two series are physically related we would expect a consistent or slowly varying phase lag. On the other hand, WTC can be thought of as the local correlation between two CWTs. In this way, locally phase locked behavior is uncovered. The more desirable features of the WTC come at the price of being slightly less localized in time frequency space.

2.3.1 Significant Wavelet Coherence

The confidence levels for the cross wavelet spectrum can be derived from the square root of the product of two chi-square distributions (Jenkins and Watts, 1968; Torrence and Compo, 1998). If the two series have theoretical Fourier spectra B_s^X and B_s^Y, then the cross wavelet distribution is:

$$\frac{W_n^X(s)W_n^{Y*}(s)}{\sigma_X \sigma_Y} \Rightarrow \frac{Z_v(p)}{v}\sqrt{B_s^X B_s^Y} \tag{11}$$

where σ_X and σ_Y are the respective standard deviations and v equals to 1 ($Z_1(95\%)=2.182$) or 2 ($Z_2(95\%)=3.999$) for real and complex wavelets, respectively.

In order to apply these ideas on real EEG signals one may define population specific background spectra for each channel pair (X, Y) and scale index s. Here again the background spectra or control-task spectra are defined as the mean time-averaged wavelet power spectrum for each channel and scale ($\overline{W}^X(s)$ and $\overline{W}^Y(s)$), which in the case of

population based analyses could be the average power spectrum over all subjects performing the control task (Sakkalis et al., 2006b). Hence, by calculating both background spectrums ($\overline{W}^{X}(s)$ and $\overline{W}^{Y}(s)$) for a pair of channels and setting $Z_v(p)=Z_2(p)=3.999$, since Morlet is a complex mother wavelet, one is able to define the background spectrum using equation 11.

However, in order to gain confidence in the interdependencies of the coherence findings one should estimate the statistical level of significance against a background spectrum using Monte Carlo methods (Grinsted et al., 2004). To adapt this idea to EEG signals one can generate a large (order of 1000) ensemble of mean time-averaged wavelet power spectrum for each channel and scale ($\overline{W}^{X}(s)$ and $\overline{W}^{Y}(s)$) using the bootstrap resampling procedure (You actually randomize the time signatures of each coherence measure). Then, for each pair of channels and each scale the wavelet coherence is calculated. Finally, the probability distribution of the calculated coherence values is used to define the 95% confidence level. After that one is able to indicate significant regions over the time-scale transform by contours (depicted in green dashed lines in Fig. 1).

Having derived this significant information, we are now able to form a single measure per scale which reflects the Significant Coherence. We are able to obtain the coherence values over those time- and band-localized regions where significant coherence is indicated by taking the coherence averages over certain bands and significant time points (contours in Fig. 1). An interesting study that successfully utilizes the latter approach in extracting the variability of neural interconnections in schizophrenia patients as compared to healthy ones is underlined in (Sakkalis et al., 2006a).

2.3.2 Partial Directed Coherence (PDC)

Extending interdependence methods to causal interaction relationship one should initially refer to the concept of Granger-causality (Granger, 1969), which is based on the commonsense idea that causes precede their effects in time and is formulated in terms of predictability. In a linear framework, Granger-causality is commonly evaluated by fitting Vector Autoregressive Models. Suppose that a set of N simultaneously observed time series $\mathbf{x}(t) = \left[x_1(t), ..., x_N(t) \right]^T$ is adequately represented by a Vector Autoregressive Model of order p (MVAR(p)):

$$\mathbf{x}(t) = \sum_{k=1}^{p} A_k \mathbf{x}(t-k) + \mathbf{w}(t) \tag{12}$$

where $\mathbf{A}_k = \begin{bmatrix} a_{11}(k) & \cdots & a_{1N}(k) \\ \vdots & \ddots & \vdots \\ a_{N1}(k) & \cdots & a_{NN}(k) \end{bmatrix}$ is the coefficient matrix at time lag k, and

$\mathbf{w}(t) = \left[w_1(t), ..., w_N(t) \right]^T$ is the vector of model innovations having zero mean and covariance matrix Σ_w. The autoregressive coefficients $a_{ij}(k)$, $i,j=1,..., N$ represent the linear interaction effect of $x_j(t-k)$ onto $x_i(t)$. In order to provide a frequency domain description of Granger-causality, Baccala and Sameshima (Baccala and Sameshima, 2001) introduced the concept of

Partial Directed Coherence (PDC), which has recently been generalized to the new PDC (Baccala et al., 2007), as follows:

Let
$$A(\lambda) = \sum_{k=1}^{p} A_k e^{-i 2 \pi \lambda k} \tag{13}$$

be the Fourier transform of the coefficient matrices, where λ is the normalized frequency in the interval [-0.5,0.5] and $i = \sqrt{-1}$. Then the new PDC is defined (Baccala et al., 2007) as:

$$\left| \pi_{i \leftarrow j}(\lambda) \right| = \frac{\dfrac{1}{\sigma_i} \left| \overline{A}_{ij}(\lambda) \right|}{\sqrt{\displaystyle\sum_{m=1}^{p} \dfrac{1}{\sigma_m^2} \overline{A}_{mj}(\lambda) * \overline{A}_{mj}^{H}(\lambda)}} \tag{14}$$

where $\overline{A}(\lambda) = I - A(\lambda)$ and σ_i^2 refers to the variance of the innovation processes $w_i(t)$. $\left| \pi_{i \leftarrow j}(\lambda) \right|$ ranges between 0 (indicating independence) and 1 (indicating maximum coherence). The latter is a linear method able to assess not only the independence of the brain regions, but also the direction of the statistically significant relationships. This method along with nonlinear ones (will be presented next) was successfully applied in studying the brain activity based on its independent components instead of the EEG signal itself. Both linear and nonlinear synchronization measures are applied to EEG components, which are free of volume conduction effects and background noise (Sakkalis et al., 2008b). More specifically, partial directed coherence was investigated in a working memory paradigm, during mental rehearsal of pictures.

3. Nonlinear synchronization techniques applied in EEG analysis

In the early 1980s, the notion of synchronization was extended to the case of interacting chaotic oscillators (Afraimovich et al., 1986; Fujisaka and Yamada, 1983; Pecora and Carroll, 1990; Pikovsky, 1984). A completely different approach in analyzing the nonlinear dynamics of an EEG signal started some decades after the discovery of deterministic chaos (Lorenz, 1963). According to Pikovsky et al. (2001) synchronization may be understood as an "adjustment of rhythms of oscillating objects due to their weak interaction". An interaction can be realized for instance through a unidirectional or bidirectional coupling. The latter case resembles mutual synchronization; both systems adjust their rhythms to each other, whereas the former case refers to synchronization initiated by an external force, called a driver, and the driven system is called a response. The rhythm of the response is adjusted to the rhythms of the driver. As soon as the interaction strength gets strong (very large values of coupling) one cannot speak of two interacting systems but rather of one combined system.

3.1 Phase Synchronization
Cognitive acts require the integration and constant interaction of widely distributed neuronal areas over the brain (Friston et al., 1997; Tononi and Edelman, 1998). Especially, gamma band is believed to reveal such large-scale oscillations that enter into precise phase-

locking over a limited period of time, often referred as phase-synchrony phenomena (Lachaux et al., 1999). Another example is thought to be the genesis of epileptic phenomenon, where synchrony has long been considered as an important factor (Niedermeyer and Lopes da Silva, 1999). Hence, some methods capable to obtain a statistical measure of the strength of phase synchronization in different areas of the brain have generated a lot of interest (Le Van Quyen et al., 2005; Mormann et al., 2000; Quian Quiroga et al., 2002).

One of the first experimental observations of synchronization was reported by Christiaan Huygens (1673) when two pendulum clocks hanging from the same beam got synchronized by attaining their maximal amplitudes at the same time but at opposite extremes thanks to the weak coupling provided by the vibration of the beam in response to their movement. However, these pendulum clocks were actually harmonic linear oscillators. But, it is well known at present that even the phases of two coupled nonlinear (noisy or chaotic) oscillators may also synchronize even if their amplitudes remain uncorrelated (Pikovsky et al., 2001; Rosenblum et al., 1996). The word "synchronization" arises from the Greek word "σύγχρονος", which consists of two parts: συν- (syn-=common) and χρόνος (chronos=time). Hence, this word is capable of describing any phenomena that "happen at the same time".

The calculation of phase synchronization (PS) and specifically instantaneous phase calculation can be based on both the Hilbert (HT) (Le Van Quyen et al., 2005; Quian Quiroga et al., 2002) or wavelet transform (WT) (Le Van Quyen et al., 2005). Actually both approaches are essentially equivalent (Quian Quiroga et al., 2002). The main difference is that the HT needs band-pass pre-filtering (Angelini et al., 2004; Bhattacharya and Petsche, 2001; Koskinen et al., 2001), whereas WT do not, since filtering is intrinsic in the WT. The most commonly used approach among the two utilizes the HT. Hence, HT is involved in getting the analytical signal $A(t)$:

$$A(t) = x(t) + i\tilde{x}(t) \tag{15}$$

where $\tilde{x}(t)$ is the HT of the signal $x(t)$, defined as:

$$\tilde{x}(t) = \frac{1}{\pi} P \int_{-\infty}^{\infty} \frac{x(\tau)}{t - \tau} d\tau \tag{16}$$

with P denoting the Cauchy principal value. The instantaneous phase is the "unfolded" angle of the analytic signal, which is given by:

$$\phi(t) = \arctan \frac{\tilde{x}(t)}{x(t)} \tag{17}$$

Synchronization of noisy signals is marked by an appearance of horizontal plateaus in the phase difference across time. The phase synchronization is defined as the locking of the phases of two oscillating systems x and y at any time t:

$$\phi_{n,m}(t) = \left| n\phi_x(t) - m\phi_y(t) \right| \le const \tag{18}$$

where $\phi_x(t)$ and $\phi_y(t)$ are the unwrapped phases of the signals associated to each system.

In this case, as we aim to measure the synchronization between signals from within the same physiological system (i.e., the brain), we assume the phase locking ratio of n:m=1:1 as per Mormann et al. (2000).

Moreover, to quantify the strength of phase synchronization, we need to choose among a number of phase indices that have been used for intracranial and scalp EEG, such as Shannon entropy (Quian Quiroga et al., 2002) and phase locking value (PLV) (Lachaux et al., 1999; Le Van Quyen et al., 2005; Mormann et al., 2000; Quian Quiroga et al., 2002). The latter, which is also termed as mean phase coherence or synchrony factor (Tallon-Baudry et al., 2001), has been found to be more robust than the alternatives especially when applied to a low number of data samples (Quian Quiroga et al., 2002). Thus, it is an optimal choice when used for scalp EEG (Garcia Dominguez et al., 2005); thus was opted in our applications (Sakkalis et al., 2009).

$$PLV = \left| \left\langle e^{i\phi(t)} \right\rangle \right| = \left| \frac{1}{N} \sum_{j=0}^{N-1} e^{i[\phi_x(j\Delta t) - \phi_y(j\Delta t)]} \right| \tag{19}$$

where $\langle \cdot \rangle$ denotes the average over time and N is the time series. This can be expanded according to Euler's formula as follows:

$$PLV = \sqrt{\left(\frac{1}{N} \sum_{j=0}^{N-1} \sin[\phi_x(j\Delta t) - \phi_y(j\Delta t)] \right)^2 + \left(\frac{1}{N} \sum_{j=0}^{N-1} \cos[\phi_x(j\Delta t) - \phi_y(j\Delta t)] \right)^2} \tag{20}$$

Hence, PLV is a normalized value which in simpler words measures how the relative phase is distributed over the unit circle. In case of perfect synchronization the relative phase will occupy a small portion of the circle and PLV will be close to a value of 1, whereas when PLV has a value close to 0, relative phases spread out over the entire unit circle and the mean phase coherence is low.

Important notes and applications

Many studies have attempted to study synchronization based on the traditionally formulated coherence. However, PLV is more suited mainly because of the following reasons (coherence limitations):

- *Stationarity*: Coherence may be applied only to stationary signals. In EEG the assumption of stationarity is rarely met or validated. PLV on the other hand does not require any stationarity.
- *Strictly phase specific measurements*: Coherence also increases with amplitude covariance and the relative importance of amplitude and phase covariance in the coherence value is not clearly justified. However, since phase-locking on its own is adequate to indicate brain lobe interactions, PLV is superior because it is only based on the phase and does not consider the amplitude of the signals.

A number of key works in the field demonstrate the applicability of phase synchronization method especially in combination with the gamma frequency band. Synchronization in the gamma band of the EEG is thought to reflect the appearing of an integrative mechanism bringing together widely distributed sets of neurons to effectively carry out different cognitive tasks (Bendat and Piersol, 1993; Tallon-Baudry et al., 2001; Varela et al., 2001). Rodriguez et al. (1999) found increased PS with a latency of 260 ms after the stimulus in the frequency range between 35 and 45 Hz in a group of adult human subjects during visual perception of faces, as opposed to the no-perception situation. Phase synchrony has been found also during non-visual perception but in a different frequency band (Trujillo et al., 2005). Another interesting result reported by Rodriguez et al. (1999) is the existence of a

period of strong desynchronization with latency between 400 and 650 ms after the stimulus, which reflects the active uncoupling of the neural ensembles necessary to proceed from the visual perception cognitive state to the motor activation state (Rodriguez et al., 1999; Varela et al., 2001). Schnitzler and Gross (2005) have reviewed the latest findings on the concept of long-range neuronal synchronization and desynchronization in motor control and cognition, in normal as well as pathological conditions.

Phase synchrony and gamma desynchronization reflects the successful formation of declarative memory, as demonstrated by the analysis of the relationship between human EEGs from the hippocampus and the rhinal cortex (Fell et al., 2001). Fell et al. (2003) concluded that, whereas rhinal-hippocampal gamma EEG PS may be closely related to actual memory processes, by enabling fast coupling and decoupling of the two structures, theta coherence might be associated with slowly modulated coupling related to an encoding state.

3.2 Generalized Synchronization

Chaotic systems appear to have an apparently noisy behavior, which in fact is ruled by deterministic laws. In a purely deterministic system once its present state is fixed, the states of all future times are determined as well. Deterministic chaos is characterized by sensitivity to initial conditions, which means that trajectories starting from very close points may give results that diverge exponentially after some time. Non linear neural time series analysis was motivated by the fact that many crucial neural processes enclose nonlinear characteristics, i.e. the regulation of voltage-gated ion channels corresponds to a steep nonlinear step-function relating membrane potential to current flow. Human EEG data was reported to exhibit chaotic dynamics in waking states (Accardo et al., 1997; Mayer-Kress and Layne, 1987; Pritchard and Duke, 1992) and in the alpha rhythm (Gallez and Babloyantz, 1991; Soong and Stuart, 1989). In addition, chaotic descriptors like the fractal dimension of the EEG were found to change through the different sleep stages (Fell et al., 1993) and during the performance of various cognitive tasks (Gregson et al., 1990; Lutzenberger et al., 1992). However, even if neurons are highly nonlinear devices, further studies did not find any strong evidence of chaos in EEG (Theiler and Rapp, 1996). Hence, at present there is a wide consensus that EEG signal are not (low-dimensional) chaotic (Lehnertz et al., 2000). In spite of this, nonlinear measures in EEG are still used since there is evidence that even if no chaotic behavior is mathematically evident, the use of phase space representations (see next paragraph) of the signals may reveal nonlinear structures hidden to standard linear approaches (Stam, 2005).

In a deterministic system it is important to establish a vector space, known as state space or phase space for the system such that specifying a point in this space specifies the state of the system, and vice versa. Even for nondeterministic systems the state concept is also powerful in the sense that a system maybe described by a set of states (possibly infinite) and a set of transition rules, which specify how a system proceeds from one state to the next.

After stressing the importance of phase space for the study of the dynamic nature of a deterministic system, there is a need to link this concept with experiments where one acquires time series and not phase space portraits. We therefore need to convert the time series samples observations into state vectors. This problem of state space reconstruction is solved by the method of delays (Takens, 1980).

If we consider the time series to be xn then a delay reconstruction vector in m dimensions is formed by the vectors:

$$\vec{x}_n = (x_n, x_{n-\tau}, \ldots, x_{n-(m-2)\tau}, x_{n-(m-1)\tau}) \tag{21}$$

where $n=1,\ldots,N$ (N equals the signal length), m is the embedding dimension and τ denotes the delay time or lag. Note that for $\tau > 1$, only the time window covered by each vector is increased, while the number of vectors constructed from the scalar time series remains roughly the same. This is because we create a vector for every scalar observation, with $n>(m-1)\tau$. Finding a good embedding is always a matter of great concern and is related to the proper selection of the embedding dimension m and the time lag τ. The right parameter selection depends on the underlying dynamics in the data and on the kind of the analysis intended. Generally, these parameters are optimized by either using statistics for their determination (Cao, 1997), or by starting the intended analysis right away and further increasing the values of m and τ until the results are optimized. A precise knowledge of m is beneficial in order to exploit determinism with minimal computational cost and no redundancy. On the other hand a good estimate of the time lag τ is more difficult to obtain. If τ is too small compared to the internal time scales of the system under consideration, successive elements of the delay vectors are strongly correlated. On the contrary, if τ is very large, successive elements are already almost independent. However, the first zero of the autocorrelation function of the signal often yields a good trade-off between the former extreme cases.

The simplest form of synchronization occurs if the states of systems exactly coincide in time. This type of synchronization is usually referred to as identical synchronization. It can be observed if the coupling strength between identical systems is high enough (Pikovsky, 1984). Two systems X and Y with state vectors $\vec{x}(t)$ and $\vec{y}(t)$ are identically synchronized ($X \Leftrightarrow Y$) if:

$$\lim_{t \to \infty}[\vec{x}(t) - \vec{y}(t)] = 0 \tag{22}$$

In order to achieve identical synchronization the parameters of the coupled systems must be identical. Otherwise, even if there is a slight mismatch the states of the systems may come close but still remain different. Obviously, identical synchronization is defined in a conceptual basis. In practice, even if the systems are not identical, weaker synchronization is possible when one system (response) is driven by the other (driver). This phenomenon is characterized as generalized synchronization (Pecora and Carroll, 1990; Rulkov et al., 1995) and is met if the state of the response $\vec{y}$ is completely defined by the state of the driver $\vec{x}$ ($X \to Y$). Hence, there exists a transformation function G such that:

$$\vec{y} = G(\vec{x}) \tag{23}$$

Strong or weak synchronization is realized in the case of smooth or non-smooth transformation function (Hunt et al., 1997; Pyragas, 1996). Rulkov et al. (1995) defined this function to be continuous one-to-one, meaning that not only the response orbit may be predicted by the driver's orbit, but also the neighborhoods in the driver space are mapped into the neighborhoods of the response space. The latter property is extensively utilized for experimental purposes.

Important concerns

Phase synchronization and generalized synchronization are not clearly related. Initially, the phase synchronization was found to appear before the generalized synchronization pops in and as a result it was thought that generalized synchronization implies phase synchronization. However, later studies on several examples had shown the reverse order (Zheng and Hu, 2000). Another thought was to apply generalized synchronization methodologies to the phases of the systems rather than the systems themselves (Lee et al., 2003). The latter is often described as generalized phase synchronization.

A challenging application for measures of synchronization is the study of neuronal dynamics, since synchronization phenomena have been increasingly recognized as a key feature for establishing the communication between different regions of the brain (Fell et al., 2001; Varela et al., 2001). Pathological cases such as Parkinson's disease or epilepsy have also taken advantage of synchronization methods in revealing synchronization and desynchronization events. Especially, when epilepsy patients undergo pre-surgical diagnostics (Lopes da Silva, 1999), intracranial recordings are acquired in order to provide sufficient localization information for the epileptic focus in the brain. This motivated us to carry out a comprehensive comparison of different measures of synchronization, as presented in Sakkalis et al. (2009).

In the experimental setting the instantaneous states of a neurophysiological process and system are not accessible. However, considering that scalp EEG is able to provide us a set of m channels equation 23 may be extended as:

$$y_j(t) = G(\vec{x}_s(t)) + \varepsilon_j(t), \quad j = 1, 2, \ldots, m \tag{24}$$

where $\varepsilon_j(t)$ denotes extraneous noise. In the simplest case, the transformation function G may be a linear superposition of a subset (denoted as s) of the $\vec{x}_s$ (such as the oscillating membrane potentials), or may involve a more complex transformation. However, the primary aim of interdependence analysis is not to recover the underlying dynamics, but only to determine whether there is nonlinear interdependence between the observables y_j due to nonlinear interdependence between the local subsystems $\vec{x}_s$.

In brief, synchronization measures quantify how well the phase space trajectory can be predicted, knowing the trajectory of the other. Clearly, such an attempt makes sometimes easier or more difficult to predict the own dynamics of each system alone. Schiff et al. (1996) initially developed the first algorithm that exploited such considerations and demonstrated nonlinear interdependence in a spinal cord preparation. The idea was to first locate the k-nearest neighbors of each point along an orbit in one phase space and then project these points into the other state space. Next, the center of the resulting cloud of projected points is used to predict the state of that system. Finally, the Euclidean distance between the predicted and observed vectors yields an error, which is then normalized by reference to a randomly chosen vector (the predicted error is, on average, no closer than random to the observed vector). The minimum error value of 0 or the maximum of 1 are taken when the systems experience maximum interdependence or when the systems are completely independent, respectively. Variants of this idea have been proposed in order to improve predictions (Feldmann and Bhattacharya, 2004; Terry and Breakspear, 2003).

Alternatively, another set of in principle more robust measures have been proposed, where instead of looking for predictions one quantifies how neighborhoods in one attractor maps into the other. In the following section this kind of algorithms will be discussed thoroughly.

Arnhold et al. (1999) similarly use k-nearest neighbors, but calculate the average radius of the cloudlike region formed by these neighbors. The ratio of the cloudlike radius to that of the cloud in the other system's reconstructed phase space defines a measure of system interdependence. This idea turned out to be a robust and reliable way of assessing the extent of GS (Sakkalis et al., 2009; Schmitz, 2000).

First, we reconstruct delay vectors (Takens, 1980) out of our time series;

$$x_n = (x_n, \ldots, x_{n-(m-1)\tau}) \text{ and } y_n = (y_n, \ldots, y_{n-(m-1)\tau}) \tag{25}$$

where $n=1\ldots N$, and m, τ are the embedding dimension and time lag, respectively. Let $r_{n,j}$ and $s_{n,j}$, $j=1,\ldots,k$, denote the time indices of the k nearest neighbors of x_n and y_n, respectively. For each x_n the mean squared Euclidean distance to its k neighbours (blue arrows, Fig. 2) is defined as:

$$R_n^{(k)}(X) = \frac{1}{k} \sum_{j=1}^{k} (\mathbf{x}_n - \mathbf{x}_{r_{n,j}})^2 \tag{26}$$

and the Y-conditioned squared mean Euclidean distance $R_n^{(k)}(X|Y)$ is defined by replacing the nearest neighbors by the equal time partners of the closest neighbors of y_n (red arrows, Fig. 2):

$$R_n^{(k)}(X|Y) = \frac{1}{k} \sum_{j=1}^{k} (\mathbf{x}_n - \mathbf{x}_{s_{n,j}})^2 \tag{27}$$

If the set of reconstructed vectors (point cloud x_n) has an average squared radius $R(X) = (1/N) \sum_{n=1}^{N} R_n^{(N-1)}(X)$, then $R_n^{(k)}(X|Y) \approx R_n^{(k)}(X) << R(X)$ if the systems are strongly correlated, while $R_n^{(k)}(X|Y) \approx R(X) >> R_n^{(k)}(X)$ if they are independent. Hence, an interdependence measure $S^{(k)}(X|Y)$ is defined as (Arnhold et al., 1999):

$$S^{(k)}(X|Y) = \frac{1}{N} \sum_{n=1}^{N} \frac{R_n^{(k)}(X)}{R_n^{(k)}(X|Y)} \tag{28}$$

Since $R_n^{(k)}(X|Y) \geq R_n^{(k)}(X)$ by construction, it is clear that S ranges between 0 (indicating independence) and 1 (indicating maximum synchronization).

Following equation 28 another nonlinear interdependence measure $H^{(k)}(X|Y)$ is possible to be defined as (Arnhold et al., 1999; Quian Quiroga et al., 2000):

$$H^{(k)}(X|Y) = \frac{1}{N} \sum_{n=1}^{N} \log \frac{R_n(X)}{R_n^{(k)}(X|Y)} \tag{29}$$

This is zero if X and Y are completely independent, while it is positive if nearness in Y implies also nearness in X for equal time partners. It would be negative if close pairs in Y would correspond mainly to distant pairs in X. This measure if applied to coupled chaotic systems was found to be robust against noise (Quian Quiroga et al., 2000), but with the drawback that it is not normalized.

Hence, another normalized and more robust version of S maybe defined as in equation 30 (Quian Quiroga et al., 2002) and is the one actually used in our work (Sakkalis et al., 2009):

$$N^{(k)}(X|Y) = \frac{1}{N} \sum_{n=1}^{N} \frac{R_n(X) - R_n^{(k)}(X|Y)}{R_n(X)} \qquad (30)$$

In fact, all three measures described are just different ways of normalizing the point cloud ratio of distances.

The opposite interdependences $S^{(k)}(Y|X)$, $H^{(k)}(Y|X)$ and $N^{(k)}(Y|X)$ are defined in complete analogy but in general are not equal to $S^{(k)}(X|Y)$, $H^{(k)}(X|Y)$ and $N^{(k)}(X|Y)$, respectively. However, this asymmetry as opposed to other symmetrical nonlinear measures such as the phase synchronization may be advantageous, since it can give information about driver response relationships (Arnhold et al., 1999; Quian Quiroga et al., 2000; Schmitz, 2000). A schema representing the idea of this algorithm is represented in figure 2.
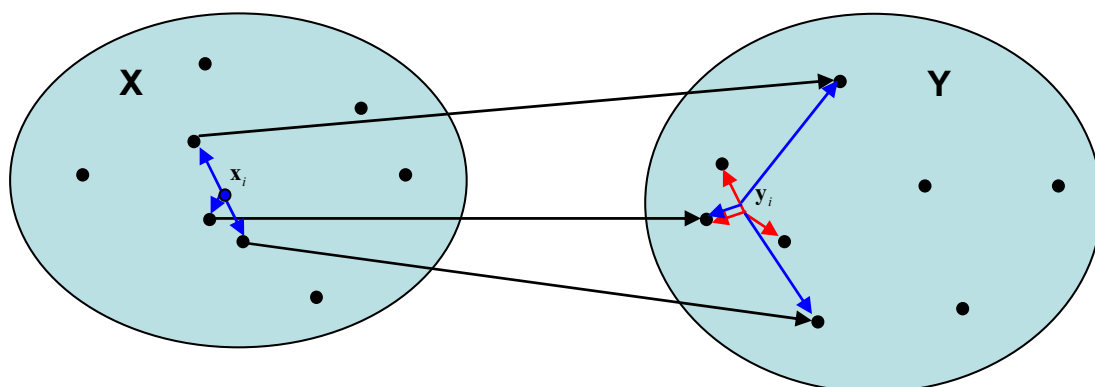
Fig. 2. Scheme representation of the basic idea of the synchronization method described by Arnhold et al. (1999). The blue and red arrows reflect an exemplar case of three nearest neighbors of x_i and y_i, respectively. The black arrows denote the respective positions of the neighbors of x_i in the Y domain.

Stam & van Dijk (2002) proposed a method which, by normalizing to a reference neighborhood, yields a synchronization likelihood (SL) measure that is not biased by the dimension of the systems' phase spaces (which are not necessarily equal). It is closely related to the previous idea and represents a normalized version of mutual information.
Supposing that x_i, x_j and y_i, y_j be the time delay vectors, SL actually expresses the chance that if the distance between x_i and x_j is very small (bounded by the white circular area in Fig. 3), the distance between the corresponding vectors y_i and y_j in the state space will also be very small. For this, we need a small critical distance ε_x, such that when the distance between x_i and x_j is smaller than ε_x, x will be considered to be in the same state at times i and j. ε_x is chosen such that the likelihood of two randomly chosen vectors from x (or y) will be closer than ε_x (or ε_y) equals a small fixed number p_{ref}. p_{ref} is the same for x and y, but ε_x need not be equal to ε_y. Now SL between x and y at time i is defined as follows:

$$SL_i = \frac{1}{N'} \sum_{\substack{j=1 \\ w_1 < |i-j| < w_2}}^{N'} \theta(\varepsilon_{y,i} - |\mathbf{y}_i - \mathbf{y}_j|)\theta(\varepsilon_{x,i} - |\mathbf{x}_i - \mathbf{x}_j|) \tag{31}$$

Here, $N'=2(w_2-w_1-1)P_{ref}$, $|\cdot|$ is the Euclidean distance and θ is the Heaviside step function, $\theta(x)=0$ if $x \le 0$ and $\theta(x)=1$ otherwise. w_1 is the Theiler correction for autocorrelation effects and w_2 is a window that sharpens the time resolution of the synchronization measure and is chosen such that $w_1 \ll w_2 \ll N$ (Theiler, 1986). When no synchronization exists between x and y, SL_i will be equal to the likelihood that random vectors y_i and y_j are closer than ε_y; thus $SL_i=p_{ref}$. In the case of complete synchronization $SL_i =1$. Intermediate coupling is reflected by $p_{ref} < SL_i <1$. Finally, SL is defined as the time average of the SL_i values.
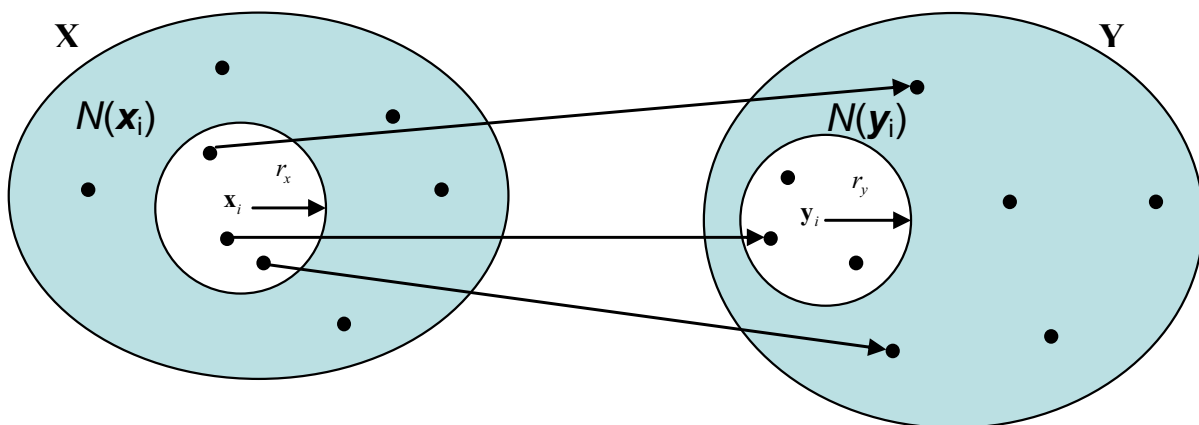
Fig. 3. Scheme representation of the basic idea of the synchronization method described by Stam et al. (2002). SL expresses the chance that if the distance between x_i and x_j (neighboring delay vectors) is less than r_x, the distance (r_y) between the corresponding vectors y_i and y_j in the state space will also be very small.

4. Surrogate time series analysis

So far we have discussed about linear and nonlinear methods for detecting synchronization in bivariate EEG signals. But how can one decide on whether a linear or nonlinear model better describes the data under study? A possible answer lies in the surrogate data testing method. In other words, to demonstrate that the synchronization methods addressed are sensitive in detecting nonlinear structures and thus reliable, surrogate data testing is used. The surrogate data method was introduced about a decade ago and the basic idea is to compute a nonlinear statistic Q for the original data under study, as well as for an ensemble of realizations of a linear stochastic process, which mimics "linear properties" of the studied data the surrogate data (Theiler, Eubank et al. 1992). If the computed nonlinear statistic for the original dataset is significantly different from the values obtained from the surrogate set, one can infer that the data is not generated by a linear process; otherwise the null hypothesis, that a linear model fully explains the data is accepted.

The surrogating procedure preserves both the autocorrelation of the signals and their linear cross-correlation, but the nonlinear individual structure of the individual signals, as well as their nonlinear interdependence, if any, is destroyed. This simply means that an ensemble of

"surrogate data" has the same linear characteristics (power spectrum and coherence) as the experimental data, but is otherwise random.

In practice, a set of p time series (surrogates) is constructed, which share the same characteristics, but lack the property we want to test, the nonlinearity in our case. Using the newly created surrogates the same index $Q_{surrogates}$ is repeatedly calculated leading to $p+1$ estimations of this. This procedure allows testing of the null hypothesis H_0 that the original value of the statistic belongs to the distribution of the surrogates, hence H_0 is true. In other words, one has to determine whether H_0 can be rejected at the desired level of confidence. By estimating the mean and the standard deviation of the distribution of the statistic from the surrogates and then comparing them with its value from the original signals Z-score is calculated:

$$Z = \frac{\left| Q - \overline{Q}_{surrogates} \right|}{\sigma_{surrogates}}$$

(32)

Z-score reveals the number of standard deviations Q is away from the mean Qs of the surrogates. Assuming that Q is approximately normally distributed in the surrogates ensemble, H_0 is rejected at the $p<0.05$ significance level when $Z>1.96$ (one-sided test). If, in addition, no other possible causes of such a result can be accounted for, then it is reasonable to conclude that the tested measure accounts for any nonlinear phenomena.

However, it should be noted that, although the above surrogating procedure preserves both the autocorrelation of the signals and their linear cross-correlation, the nonlinear individual structure of the individual signals, if any, is also destroyed. In other words, any nonlinearity not only between but also within the signals is not present in the surrogates. Therefore, these surrogates only test the hypothesis that the data are bivariate stochastic time series with an arbitrary degree of linear auto and cross-correlation (Andrzejak, Kraskov et al. 2003). Nevertheless, if the two signals studied do have any nonlinear structure, it is not possible to ascribe a rejection of the hypothesis that the interdependence is nonlinear due to the nonlinearity of the interdependence, because the nonlinearity of the individual signals may also play a role. Hence, the generation of surrogate data preserving all the individual structure but destroying only the nonlinear part of the interdependence is currently one of the most challenging tasks in the field, and it is a subject of ongoing research (Andrzejak, Kraskov et al. 2003; Dolan 2004).

Pure nonlinear interdependence can contribute to linear correlations, but cannot be detected by linear methods alone. It signifies the formation of macroscopic, dynamic neural cell assemblies and transient low-dimensional interactions between them. Nonlinear interdependence informs that the underlying dynamics are governed by nonlinear processes, or that they are linear but evolving in the vicinity of a non-linear instability and driving noise. Nonlinearities generate correlations that cannot be generated by stochastic processes, such as coupling between oscillations with different frequencies (Friston 1997; Breakspear and Terry 2002).

The most widely used method to obtain surrogate data is to randomize the phases of the signal in the Fourier domain (Theiler, Eubank et al. 1992). Recent advances such as employing iterative loops (Schreiber and Schmitz 1996), simulated annealing (Schreiber 1998) and others (Schreiber and Schmitz 2000) are all aimed to improve the goodness of the fit between the linear properties of the experimental data and surrogate ensemble.

Unforunately, as noted beforehand, no surrogate technique is perfect (Schreiber and Schmitz 2000).

To conclude the whole nonlinearity section it should be stressed that even nonlinear techniques look promising one should be cautious in practice. Many findings may have been premature in that apparent nonlinear effects were in fact caused by limitations of the data such as the sample length (Ruelle 1990). During the previous years there was a general notion that EEG is chaotic, but nowadays there is a wide consensus and it is certainly no longer generally accepted that the healthy EEG is a chaotic signal.
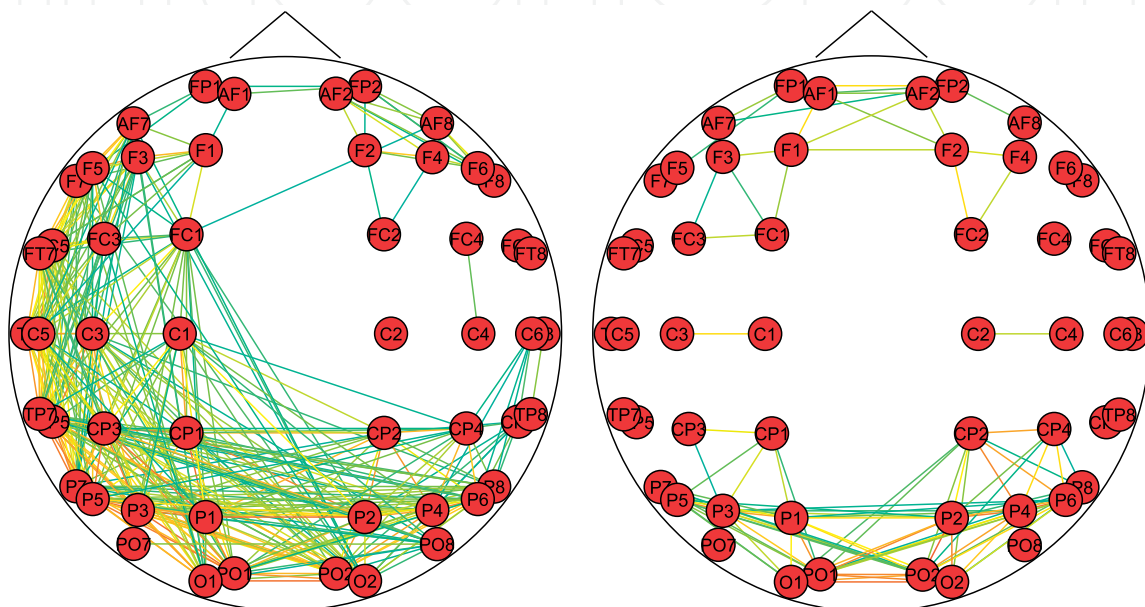
Fig. 4. A "healthy" network (left graph) appears to exhibit strong lateralization compared to the "alcoholic" one (right graph) which exhibits interhemispheric symmetry, when the broadband signals are analyzed.

5. Graph Theory in EEG analysis

An alternative approach to the characterization of complex networks is the use of graph theory (Strogatz 2001; Sporns, Chialvo et al. 2004; Sporns and Zwi 2004). A graph is a basic representation of a network, which is essentially reduced to nodes (vertices) and connections (edges) as illustrated in Fig. 4. Both local and long distance functional connectivity in complex networks may alternatively be evaluated using measures and visualizations derived from graph theory. Special interest in using graph theory to study neural networks has been in focus recently, since it offers a unique perspective of studying local and distributed brain interactions (Varela, Lachaux et al. 2001; Fingelkurts, Fingelkurts et al. 2005).

Using the interdependence methods and measures analyzed in the previous sections one is able to measure (in terms of 0 to 1) the coupling between different channels. If such interdependence measures are constructed for every possible channel pair a coherence matrix (CM) (i.e. 30x30, if 30 channels are used) with elements ranging from 0 to 1. Next, in order to obtain a graph from a CM we need to convert it into an NxN binary adjacency

matrix, A. To achieve that we define a variable called threshold T, such that $T \in [0,1]$. The value $A(i,j)$ is either 1 or 0, indicating the presence or absence of an edge between nodes i and j, respectively. Namely, $A(i,j)=1$ if $C(i,j) \geq T$, otherwise $A(i,j)=0$. Thus we define a graph for each value of T, i.e., for the purposes of our work, we defined 1000 such graphs, one for every thousandth of T (Sakkalis et al., 2006a). After constructing A, one is able to compute various properties of the resulting graph. These include the average degree K, the clustering coefficient C and the average shortest path length L of our graph, which will be presented in the next section. Figure 4 illustrates an example graph that resembles a "healthy" network (left graph) compared to the "alcoholic" one, in both broadband and lower beta frequency bands (Sakkalis et al., 2007).
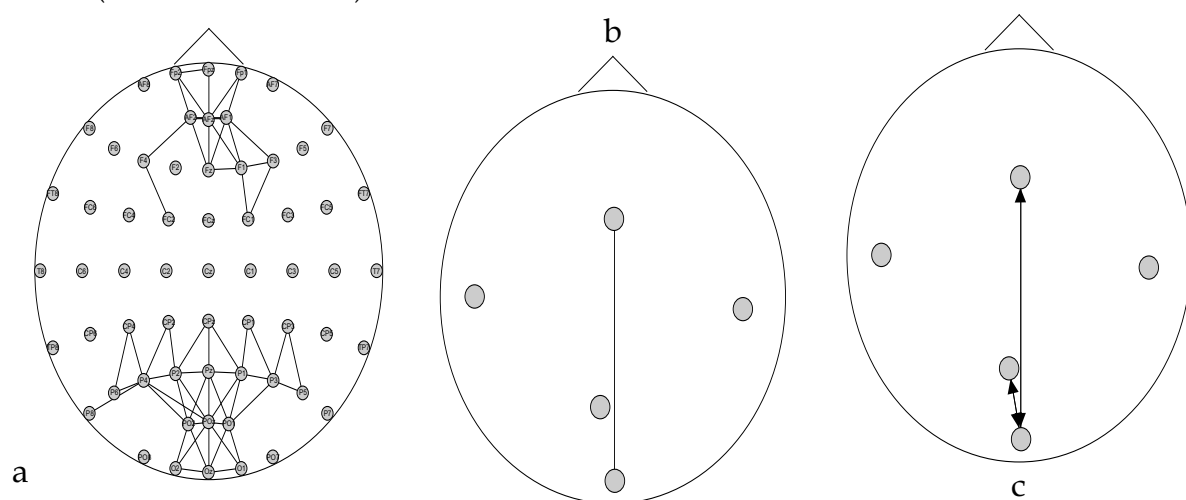
Fig. 5. a) Aerial view of the scalp with the position of electrodes. The depicted average network reflects a local prefrontal and occipitoparietal synchrony, as identified in gamma band using the nonlinear synchronization method on the actual electrode signals in a working memory paradigm. The next parts of this figure (b, c) are considering cross-regional synchrony. b) The nonlinear synchronization method is applied in gamma band ICs reflecting the underlying activity in the different brain regions (prefrontal (upper node), temporal (left and right lateral nodes), parietal (lower middle node) and occipital (lowest central node)). This figure focuses on the inter-region connectivity between the prefrontal and occipital brain areas. c) Similarly to the middle graph but using PDC; again ICs in gamma band exhibit significant linear coupling between the prefrontal and occipital areas, as well as between the occipital and parietal areas. Directionality is also identified. The apparent bidirectional coupling indicates no single influence between the "cause" and "effect" relationship. The illustrated graphs are averaged over all subjects.

Another study (Sakkalis et al., 2008b) was able to identify and visualize the established brain networks in gamma band by means of both linear and nonlinear synchrony measures, in working memory paradigm. The nonlinear GS method was initially applied on all the actual electrode recordings. The scalp map obtained (Fig. 5a) identified a network tendency to localize synchronization activity mostly at frontal and occipitoparietal regions. However, no linking between the two regions is evident. When we focus on the independent components (instead of the actual electrodes themselves), the prominent inter-region connectivity in gamma band between the prefrontal and occipital brain areas becomes evident (Fig. 5b).

Finally, a similar network topology is also derived by the linear PDC method (Fig. 5c). The latter method is able to derive additional information on the "driver and response" significant relationship between observations, denoted by arrows in Fig. 5c. However, the bidirectional arrows denote no single one-way interconnection, but a significant pathway connecting the prefrontal and occipital areas, as well as the occipital and parietal areas, is identified (Fig. 5c).

Graph theory is for sure an emerging field in EEG analysis and coupling visualization. Recent articles illustrate that graph properties maybe of particular value in certain pathologies, i.e., alcoholism (Sakkalis et al., 2007) and Alzheimer disease (Stam, Jones et al. 2006).

6. Conclusion

Throughout this chapter both linear and nonlinear interdependence measures are discussed. Even if the complex nature of EEG signals justify the use of nonlinear methods there is no evidence to support and prejudge that such methods are superior to linear ones. On the contrary, the information provided by nonlinear analysis does not necessarily coincide with that of the linear methods. In fact, both approaches should be regarded as complementary in the sense that they are able to assess different properties of interdependence between the signals. In addition the linear ones most of the times appear to be robust against noise, whereas nonlinear measures are found to be rather unstable. Stationarity is again a main concern, since it is a prerequisite which is not satisfied in practice. The selection of an adequate method will depend on the type of signal to be studied and on the questions expected to be answered. One should also bear in mind that all nonlinear methods presented require stationary signals. If this is not the case, one is better off using a linear alternative like wavelet coherence, due to its inherent adaptive windowing scaling. Another alternative is phase synchronization calculation, PLV method in specific, which requires neither stationarity nor increases with amplitude covariance like coherence. In addition, since phase-locking on its own is adequate to indicate brain lobe interactions, PLV is superior because it is only based on the phase and does not consider the amplitude of the signals. However, an interesting extension in identifying the most significant regions, in terms of increased coherence, as compared to background signals is possible using the significant wavelet coherence.

Visual ways to illustrate the results and possibly fuse them together are the topographic maps and graphs. Topographic colour maps may be used in visualizing the power spectral-based estimations, where different colourings reflect altering brain activity. In addition, interdependencies may be illustrated using graph visualizations, where channel pairwise coupling is visualized using edges of increasing thickness with respect to increasing coupling strength.

As noted throughout this chapter most of the methods presented, traditional linear or nonlinear, must assume some kind of stationarity. Therefore, changes in the dynamics during the measurement period usually constitute an undesired complication of the analysis, which in EEG may represent the most interesting structure in identifying dynamical changes in the state of the brain. Hence, a fundamental topic for further research should be the formation of a powerful test for stationarity able to indicate and reject, with increased certainty, the sections of the EEG raw signal that experience stationary behavior.

Another active research direction focuses on extending current interdependence analysis from bivariate to multivariate signals. This is important since pairwise analysis is likely to find plasmatic correlations in special cases where one driver drives two responses. In this case both responses may found to have a common driver component, even if the responses might be fully independent.

7. References

Accardo A, Affinito M, Carrozzi M, Bouquet F. Use of the fractal dimension for the analysis of EEG time series. Biol. Cybern. 1997; 77: 339-350.

Afraimovich VS, Verichev NN, Rabinovich MI. Stochastic synchronization of oscillations in dissipative systems. Radiophys. Quantum Electron. 1986; 29: 795.

Andrzejak RG, Kraskov A, Stogbauer H, Mormann F, Kreuz T. Bivariate surrogate techniques: necessity, strengths, and caveats. Phys. Rev. E 2003; 68: 066202.

Angelini L, de Tommaso M, Guido M, Hu K, Ivanov P, Marinazzo D, et al. Steady-state visual evoked potentials and phase synchronization in migraine patients. Phys Rev Lett 2004; 93: 038103.

Arnhold J, Lehnertz K, Grassberger P, Elger CE. A robust method for detecting interdependences: Application to intracranially recorded EEG. Physica D 1999; 134: 419.

Baccala L, Sameshima K, Takahashi DY. Generalized partial directed coherence. 15th Intern. Conf. Digital Signal Processing 2007, 163-166.

Baccala LA, Sameshima K. Partial directed coherence: a new concept in neural structure determination. Biological Cybernetics 2001, 84(6): 463-474.

Bhattacharya J, Petsche H. Musicians and the gamma band: a secret affair? Neuroreport 2001; 12: 371-4.

Bendat JS, Piersol AG. Engineering applications of correlation and spectral analysis. New York: J. Wiley, 1993.

Brazier MA. Spread of seizure discharges in epilepsy: anatomical and electrophysiological considerations. Exp Neurol 1972; 36: 263-72.

Brazier MA, Casby JU. Cross-correlation and autocorrelation studies of electroencephalographic potentials. Electroencephalogr Clin Neurophysiol Suppl 1952; 4: 201-11.

Cao L. Practical method for determining the minimum embedding dimension of a scalar time series. Physica D 1997; 110: 43-50.

Dolan K. Surrogate analysis of multichannel data with frequency dependant time lag. Fluct. Noise Lett. 2004; 4: L75-L81.

Dumermuth G, Molinari I. Relationships among signals: cross-spectral analysis of the EEG. In: Weitkunat R, editor. Digital Biosignal Processing. Vol 5. Amsterdam: Elsevier Science Publishers, 1991: 361-398.

Feldmann U, Bhattacharya J. Predictability improvement as an asymmetrical measure of interdependence in bivariate time series. Int. J. of Bifurcation and Chaos 2004; 14: 505-514.

Fell J, Klaver P, Elfadil H, Schaller C, Elger CE, Fernandez G. Rhinal-hippocampal theta coherence during declarative memory formation: interaction with gamma synchronization? Eur J Neurosci 2003; 17: 1082-8.

Fell J, Klaver P, Lehnertz K, Grunwald T, Schaller C, Elger CE, et al. Human memory formation is accompanied by rhinal-hippocampal coupling and decoupling. Nat Neurosci 2001; 4: 1259-64.

Fell J, Roschke J, Beckmann P. Deterministic chaos and the first positive Lyapunov exponent: a nonlinear analysis of the human electroencephalogram during sleep. Biol Cybern 1993; 69: 139-46.

Fingelkurts AA, Fingelkurts AA, Kahkonen S. Functional connectivity in the brain--is it an elusive concept? Neurosci Biobehav Rev 2005; 28: 827-36.

French CC, Beaumont JG. A critical review of EEG coherence studies of hemisphere function. Int J Psychophysiol 1984; 1: 241-54.

Friston KJ, Stephan KM, Frackowiak RSJ. Transient phase-locking and dynamic correlations: Are they the same thing? Human Brain Mapping 1997; 5: 48-57.

Fujisaka H, Yamada T. Stability theory of synchronized motion in coupled dynamical systems. Prog. Theor. Phys. 1983; 69: 32-47.

Gallez D, Babloyantz A. Predictability of human EEG: a dynamical approach. Biol. Cybern. 1991; 64: 381-391.

Garcia Dominguez L, Wennberg RA, Gaetz W, Cheyne D, Snead OCa, Perez Velazquez JL. Enhanced synchrony in epileptiform activity? Local versus distant phase synchronization in generalized seizures. J Neurosci 2005; 25: 8077-8084.

Gevins AS. Overview of computer analysis. In: Gevins AS and Rémond A, editors. Handbook of electroencephalography and clinical neurophysiology ; rev. ser., v. 1. Vol I. NY, USA: Elsevier, 1987: 31-83.

Granger J. Investigating causal relations by econometric models and cross-spectral methods. Econometrica 1969, 37(3): 424-438.

Gregson RA, Britton LA, Campbell EA, Gates GR. Comparisons of the nonlinear dynamics of electroencephalograms under various task loading conditions: a preliminary report. Biol Psychol 1990; 31: 173-91.

Grinsted A, Moore JC, Jevrejeva S. Application of the cross wavelet transform and wavelet coherence to geophysical time series. Nonlinear Processes in Geophysics 2004; 11: 561-566.

Guevara MA, Lorenzo I, Arce C, Ramos J, Corsi-Cabrera M. Inter- and intrahemispheric EEG correlation during sleep and wakefulness. Sleep 1995; 18: 257-65.

Hunt BR, Ott E, Yorke JA. Differentiable generalized synchronization of chaos. Phys. Rev. E 1997; 55: 4029-4034.

Huygens C. Horoloquium Oscilatorium. Paris, 1673.

Jenkins GM, Watts DG. Spectral Analysis and Its Applications. San Francisco, CA: Holden-Day, Inc., 1968.

Koskinen M, Seppanen T, Tuukkanen J, Yli-Hankala A, Jantti V. Propofol anesthesia induces phase synchronization changes in EEG. Clin Neurophysiol 2001; 112: 386-92.

Lachaux JP, Lutz A, Rudrauf D, Cosmelli D, Le Van Quyen M, Martinerie J, et al. Estimating the time-course of coherence between single-trial brain signals: an introduction to wavelet coherence. Neurophysiol Clin 2002; 32: 157-74.

Lachaux JP, Rodriguez E, Martinerie J, Varela FJ. Measuring phase synchrony in brain signals. Hum Brain Mapp 1999; 8: 194-208.

Lehnertz K, Arnhold J, Grassberger P, Elger C. Chaos in Brain? World Scientific. Singapore, 2000.

Le Van Quyen M, Soss J, Navarro V, Robertson R, Chavez M, Baulac M, et al. Preictal state identification by synchronization changes in long-term intracranial EEG recordings. Clin Neurophysiol 2005; 116: 559-68.

Lee D-S, Kye W-H, Rim S, Kwon T-Y, Kim C-M. Generalized phase synchronization in unidirectionally coupled chaotic oscillators. Physical Review E 2003; 67: 045201.

Lopes da Silva FH. EEG Analysis: theory and practice. In: Niedermeyer E and Lopes da Silva FH, editors. Electroencephalography : basic principles, clinical applications, and related fields. Baltimore: Williams & Wilkins, 1999: 1097-1123.

Lorenz EN. Deterministic non-periodic flow. J. Atmos. Sci. 1963; 20: 130.

Lutzenberger W, Birbaumer N, Flor H, Rockstroh B, Elbert T. Dimensional analysis of the human EEG and intelligence. Neurosci Lett 1992; 143: 10-4.

Mayer-Kress G, Layne S. Dimensionality of the human EEG. Annals New York Acad. Sci. 1987; 504: 62-87.

Mormann F, Lehnertz K, David P, Elger CE. Mean phase coherence as a measure for phase synchronization and its application to the EEG of epilepsy patients. Phys. D 2000; 144: 358--369.

Niedermeyer E, Lopes da Silva FH. Electroencephalography : basic principles, clinical applications, and related fields. Baltimore: Williams & Wilkins, 1999.

Nunez PL. Quantitative states of neocortex. In: Nunez PL, editor. Neocortical Dynamics and Human EEG Rhythms. Oxford ; New York: Oxford University Press, 1995: 33-39.

Pecora LM, Carroll TL. Synchronization in chaotic systems. Phys. Rev. Lett. 1990; 64: 821.

Pereda E, Quiroga RQ, Bhattacharya J. Nonlinear multivariate analysis of neurophysiological signals. Prog Neurobiol 2005; 77: 1-37.

Pikovsky A, Rosenblum M, Kurths J. Synchronization : a universal concept in nonlinear sciences. Cambridge: Cambridge University Press, 2001.

Pikovsky AS. On the interaction of strange attractors. Z. Phys. B: Condens Matter 1984; 55(2): 149.

Pritchard W, Duke D. Dimensional analysis of no-task human EEG using the Grassberger-Procaccia method. Psychophysiol. 1992; 29: 182-192.

Pyragas K. Weak and strong synchronization of chaos. Phys. Rev. E 1996; 54: 4508-4511.

Quian Quiroga R, Arnhold J, Grassberger P. Learning driver-response relationships from synchronization patterns. Physical Review E 2000; 61: 5142.

Quian Quiroga R, Kraskov A, Kreuz T, Grassberger P. Performance of different synchronization measures in real data: a case study on electroencephalographic signals. Phys Rev E Stat Nonlin Soft Matter Phys 2002; 65: 041903.

Rosenblum MG, Pikovsky AS, Kurths J. Phase synchronization of chaotic oscillators. Physical Review Letters 1996; 76: 1804-1807.

Ruelle D. Deterministic chaos: The science and the fiction. Proc. of the Royal Society of London 1990; 427A: 241-248.

Rulkov NF, Sushchik MM, Tsimring LS, Abarbanel HDI. Generalized synchronization of chaos in directionally coupled chaotic systems. Phys. Rev. E 1995; 51(2): 980-994.

Sakkalis V, Giurcăneanu CD, Xanthopoulos P, Zervakis M, Tsiaras V, Yang Y, Micheloyannis S. Assessment of linear and nonlinear synchronization measures for analyzing EEG in a mild epileptic paradigm. IEEE Trans. Inf. Tech. 2009; 13(4):433-441 (DOI: 10.1109/TITB.2008.923141).

Sakkalis V, Oikonomou T, Pachou E, Tollis I, Micheloyannis S, Zervakis M. Time-significant Wavelet Coherence for the Evaluation of Schizophrenic Brain Activity using a Graph theory approach. Engineering in Medicine and Biology Society (EMBC 2006). New York, USA, 2006a.

Sakkalis V, Zervakis M, Micheloyannis S. Significant EEG Features Involved in Mathematical Reasoning: Evidence from Wavelet Analysis. Brain Topography 2006b; 19: 53-60.

Sakkalis V, Cassar T, Zervakis M, Camilleri KP, Fabri SG, Bigan C, Karakonstantaki E, Micheloyannis S. Time-Frequency Analysis and Modelling of EEGs for the evaluation of EEG activity in Young Children with controlled epilepsy. Comput Intell Neurosci. CIN 2008a: 462593 (DOI: 10.1155/2008/462593).

Sakkalis V, Tsiaras V, Michalopoulos K, Zervakis M. Assessment of neural dynamic coupling and causal interactions between independent EEG components from cognitive tasks using linear and nonlinear methods. 30th IEEE-EMBS, Engineering in Medicine and Biology Society (EMBC 2008), Vancouver, Canada, August 20-24. 2008b.

Sakkalis V, Tsiaras V, Zervakis M, Tollis I. Optimal brain network synchrony visualization: Application in an alcoholism paradigm. 29th IEEE-EMBS, Engineering in Medicine and Biology Society (EMBC 2007), Lyon, France, August 23-26, 2007.

Schiff SJ, So P, Chang T, Burke RE, Sauer T. Detecting dynamical interdependence and generalized synchrony through mutual prediction in a neural ensemble. Physical Review E 1996; 54: 6708.

Schmitz A. Measuring statistical dependence and coupling of subsystems. Physical Review E 2000; 62: 7508.

Schnitzler A, Gross J. Normal and pathological oscillatory communication in the brain. Nat Rev Neurosci 2005; 6: 285-96.

Schreiber T. Constrained randomization of time series data. Phys. Rev. Lett. 1998; 80: 2105-2108.

Schreiber T, Schmitz A. Improved surrogate data for nonlinearity tests. Phys. Rev. Lett. 1996; 77: 635-638.

Schreiber T, Schmitz A. Surrogate time series. Physica, D 2000; 142: 346-382.

Shaw JC. An introduction to the coherence function and its use in EEG signal analysis. J Med Eng Technol 1981; 5: 279-88.

Shaw JC. Correlation and coherence analysis of the EEG: a selective tutorial review. Int J Psychophysiol 1984; 1: 255-66.

Soong A, Stuart C. Evidence of chaotic dynamics underlying the human alpharhythm electroencephalogram. Biol. Cybern. 1989; 42: 55-62.

Sporns O, Chialvo DR, Kaiser M, Hilgetag CC. Organization, development and function of complex brain networks. Trends Cogn Sci 2004; 8: 418-25.

Sporns O, Zwi JD. The small world of the cerebral cortex. Neuroinformatics 2004; 2: 145-62.

Stam CJ. Nonlinear dynamical analysis of EEG and MEG: review of an emerging field. Clin Neurophysiol 2005; 116: 2266-301.

Stam CJ, Jones BF, Nolte G, Breakspear M, Scheltens P. Small-World Networks and Functional Connectivity in Alzheimer's Disease. Cereb Cortex 2006.

Stam CJ, van Dijk BW. Synchronization likelihood: an unbiased measure of generalized synchronization in multivariate data sets. Physica D: Nonlinear Phenomena 2002; 163: 236-251.

Strogatz SH. Exploring complex networks. Nature 2001; 410: 268-76.

Takens F. Detecting strange attractors in turbulence. In: Rand D and Young L, editors. Dynamical Systems and Turbulence. Vol 898. Warwick: Springer-Verlag, 1980: 366-381.

Tallon-Baudry C, Bertrand O, Fischer C. Oscillatory synchrony between human extrastriate areas during visual short-term memory maintenance. J Neurosci 2001; 21: RC177.

Terry J, Breakspear M. An improved algorithm for the detection of dynamical interdependence in bivariate time-series. Biol Cybern. 2003; 88: 129-136.

Thatcher RW, Krause PJ, Hrybyk M. Cortico-cortical associations and EEG coherence: a two-compartmental model. Electroencephalogr. Clin. Neurophysiol. 1986; 64: 123-143.

Theiler J. Spurious dimension from correlation algorithms applied to limited time-series data. Phys. Rev. A 1986; 34: 2427.

Theiler J, Eubank S, Longtin A, Galdrikian B, Farmer J. Testing for nonlinearity in time series: the method of surrogate data. Physica D 1992; 58: 77-94.

Theiler J, Rapp P. Re-examination of the evidence for low-dimensional, nonlinear structure in the human EEG. Electroenceph. Clin. Neurophysiol. 1996; 98: 213-222.

Tononi G, Edelman GM. Consciousness and complexity. Science 1998; 282: 1846-51.

Torrence C, Compo G. A practical Guide to Wavelet Analysis. Bull. Am. Meteorol. Soc. 1998; 79: 61-78.

Trujillo LT, Peterson MA, Kaszniak AW, Allen JJ. EEG phase synchrony differences across visual perception conditions may depend on recording and analysis methods. Clin Neurophysiol 2005; 116: 172-89.

Varela F, Lachaux JP, Rodriguez E, Martinerie J. The brainweb: phase synchronization and large-scale integration. Nat Rev Neurosci 2001; 2: 229-39.

Zaveri HP, Williams WJ, Sackellares JC, Beydoun A, Duckrow RB, Spencer SS. Measuring the coherence of intracranial electroencephalograms. Clin. Neurophysiol. 1999; 110: 1717-1725.

Zheng Z, Hu G. Generalized synchronization versus phase synchronization. Phys. Rev. E 2000; 62: 7882-7885.

Recent Advances in Biomedical Engineering

Edited by Ganesh R Naik

The field of biomedical engineering has expanded markedly in the past ten years. This growth is supported by advances in biological science, which have created new opportunities for development of tools for diagnosis and therapy for human disease. The discipline focuses both on development of new biomaterials, analytical methodologies and on the application of concepts drawn from engineering, computing, mathematics, chemical and physical sciences to advance biomedical knowledge while improving the effectiveness and delivery of clinical medicine. Biomedical engineering now encompasses a range of fields of specialization including bioinstrumentation, bioimaging, biomechanics, biomaterials, and biomolecular engineering. Biomedical engineering covers recent advances in the growing field of biomedical technology, instrumentation, and administration. Contributions focus on theoretical and practical problems associated with the development of medical technology; the introduction of new engineering methods into public health; hospitals and patient care; the improvement of diagnosis and therapy; and biomedical information storage and retrieval. The book is directed at engineering students in their final year of undergraduate studies or in their graduate studies. Most undergraduate students majoring in biomedical engineering are faced with a decision, early in their program of study, regarding the field in which they would like to specialize. Each chosen specialty has a specific set of course requirements and is supplemented by wise selection of elective and supporting coursework. Also, many young students of biomedical engineering use independent research projects as a source of inspiration and preparation but have difficulty identifying research areas that are right for them. Therefore, a second goal of this book is to link knowledge of basic science and engineering to fields of specialization and current research. The editor would like to thank the authors, who have committed so much effort to the publication of this work.

INTECH

open science | open minds